

## Supplementary Information

### The interaction of reactants, intermediates and products with Cu ions in Cu-SSZ-13 NH<sub>3</sub> SCR catalysts: An energetic and ab initio X-ray absorption modeling study

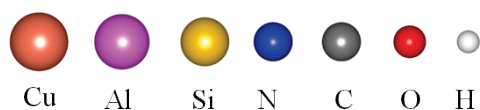
Renqin Zhang<sup>a</sup>, János Szanyi<sup>b</sup>, Feng Gao<sup>b</sup>, Jean-Sabin McEwen<sup>a,c,d\*</sup>

<sup>a</sup>*The Gene and Linda Voiland School of Chemical Engineering and Bioengineering, Washington State University, Pullman, WA 99164*

<sup>b</sup>*Institute for Integrated Catalysis, Pacific Northwest National Laboratory, Richland, WA 9935*

<sup>c</sup>*Department of Physics and Astronomy, Washington State University, Pullman, WA 99164*

<sup>d</sup>*Department of Chemistry, Washington State University, Pullman, WA 99164*



Atom legend: in this contribution, all atoms are represented as shown in this figure.

#### 1. Equilibrium volume

Equilibrium volumes for the purely siliceous chabazite as well as Al-substituted/Cu-exchanged material were described using rhombohedral unit cells and a plane-wave cutoff energy of 400 eV. The cell shape and fractional coordinates were allowed to fully relax for a sequence of volumes. In order to get an accurate equilibrium volume, we followed the step by step procedure as outlined in the VASP manual.<sup>1</sup> First, we selected one volume and relaxed the ionic position from the starting structure keeping the volume fixed (ISIF=4; ISMEAR=0). Second, we started a second ionic relaxation from the previous CONTCAR file. As a final step, we performed one more energy calculation using the tetrahedron smearing method (ISMEAR=-5), to get very accurate, unambiguous energies (no relaxation for the final run). In the first two steps of the optimization calculations, Gaussian smearing of 0.2 eV was used while the tetrahedron method with a smearing of 0.2 eV was used in the final step of energy calculation to get accurate energies. Also, these unit cells were sampled with a (3×3×3) Monkhorst-Pack k-point grids for full relaxation.

\* Corresponding author: [js.mcewen@wsu.edu](mailto:js.mcewen@wsu.edu)

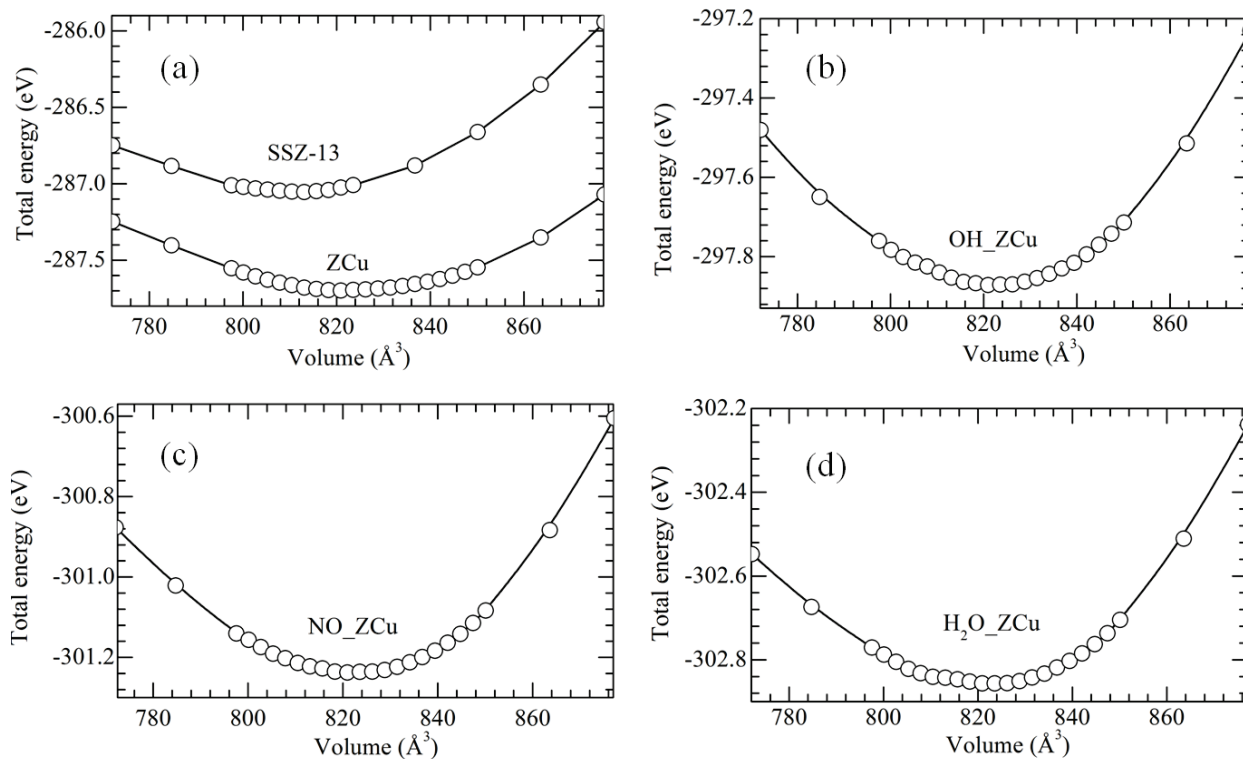


Figure S1. Plots of total energy as function of volume for SSZ-13, ZCu, and species (OH, NO, H<sub>2</sub>O) adsorbed on ZCu. The equilibrium volumes of (a) SSZ-13 and ZCu are 813.1 Å<sup>3</sup> and 823.6 Å<sup>3</sup> respectively. The equilibrium volumes of (b) OH\_ZCu, (c) NO\_ZCu and (d) H<sub>2</sub>O\_ZCu are similar to that of ZCu, which is 823.6 Å<sup>3</sup>.

## 2. The effect of unit cell and functionals on Cu K-edge XANES

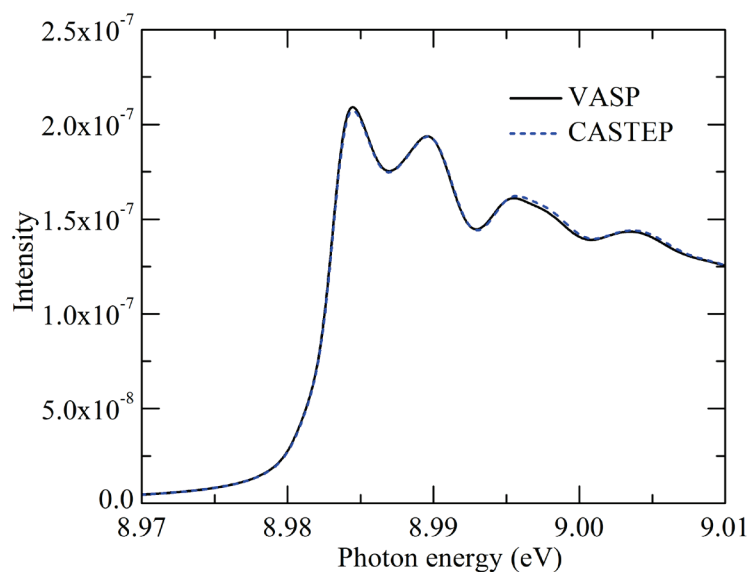


Figure S2. Cu K-edge XANES of clean ZCu with Cu in 6MR sites calculated by using the unit cell optimized within VASP (solid line) and CASTEP (dash line). By examining the figure, we can see that

the XANES spectra are the same, which implies that XANES was not affected by the optimized the unit cell within VASP and CASTEP.

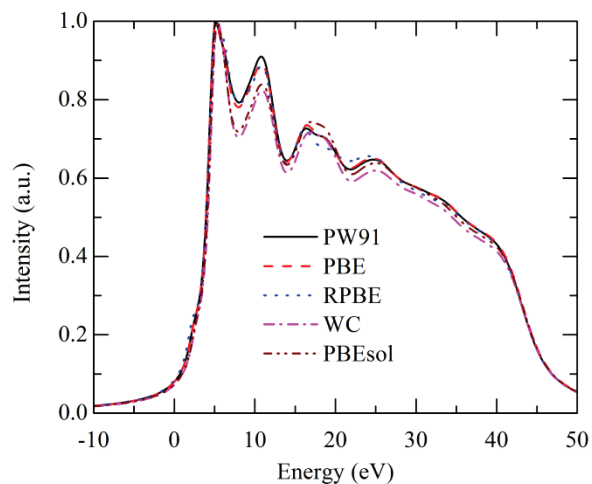


Figure S3. Theoretical K-edge XANES of Cu in ZCu with Cu in the 6MR site calculated by using different functionals, namely PW91, PBE, RPBE, WC and PBEsol, which are available in CASTEP program.

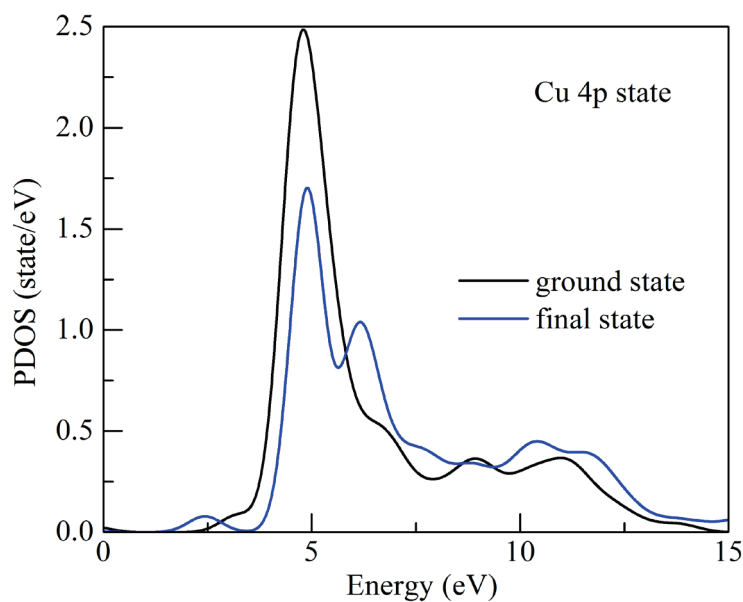
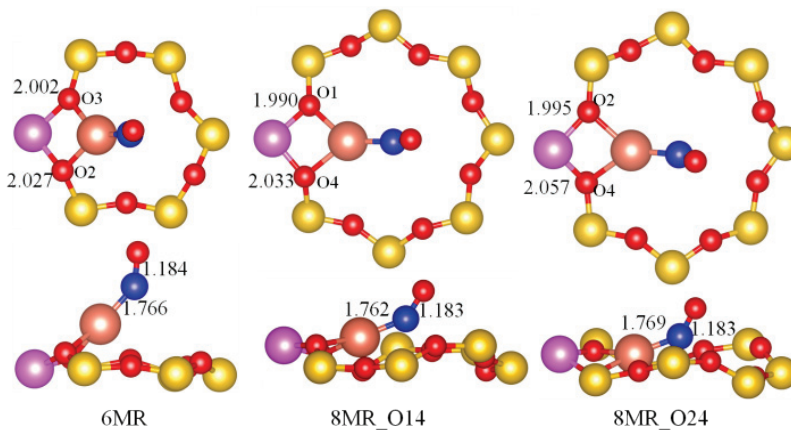


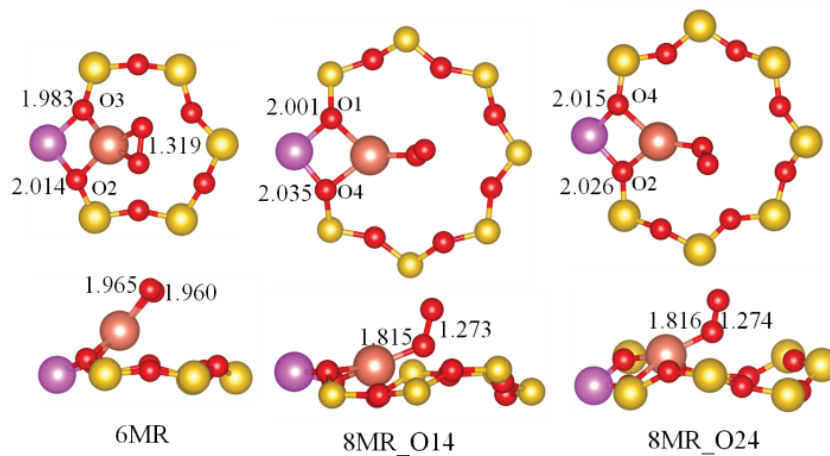
Figure S4. Comparison between the Cu 4p PDOS in its ground state and the corresponding PDOS in its final state for the clean ZCu system with Cu in a 6MR site.

### 3. Structures of molecularly adsorbed ZCu

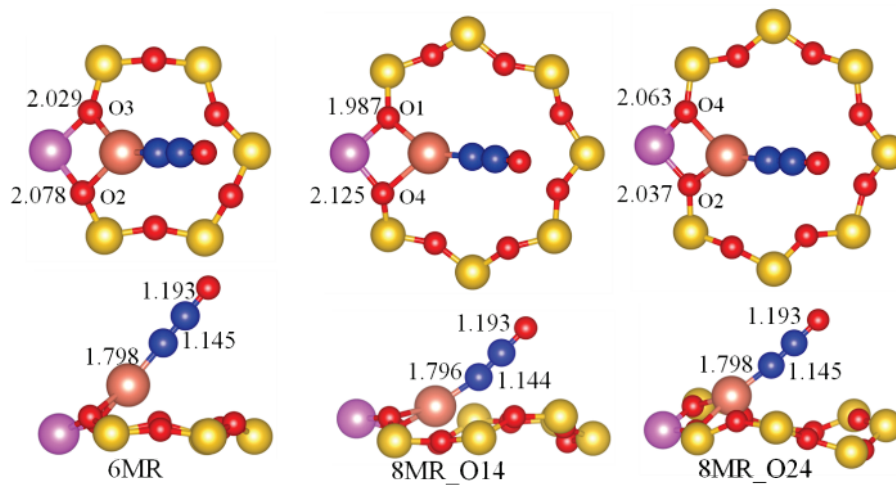
#### NO\_ZCu



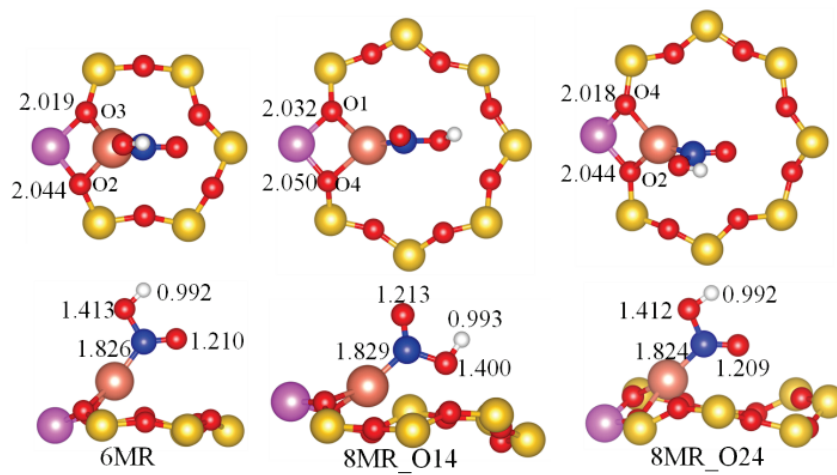
#### O<sub>2</sub>\_ZCu



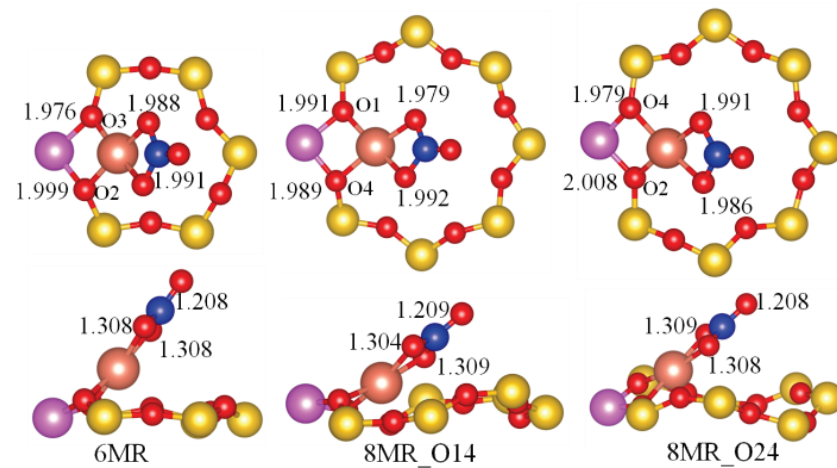
#### N<sub>2</sub>O\_ZCu



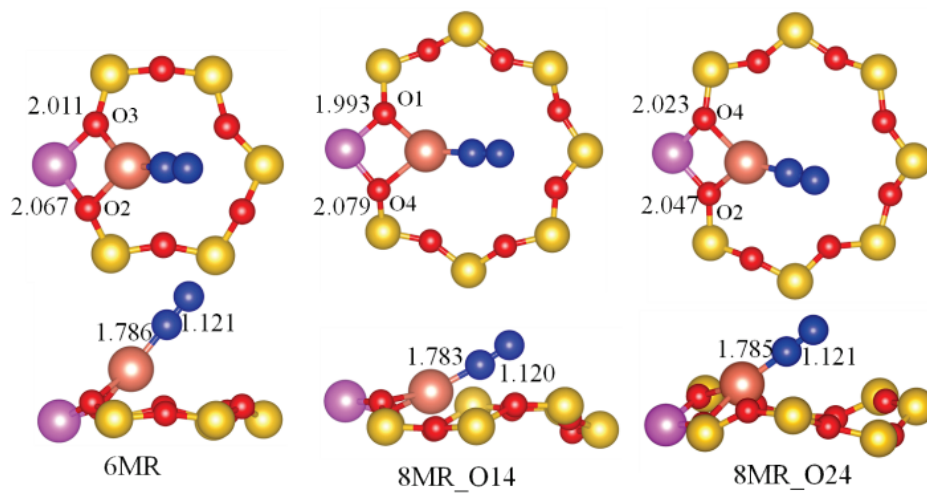
HONO\_ZCu



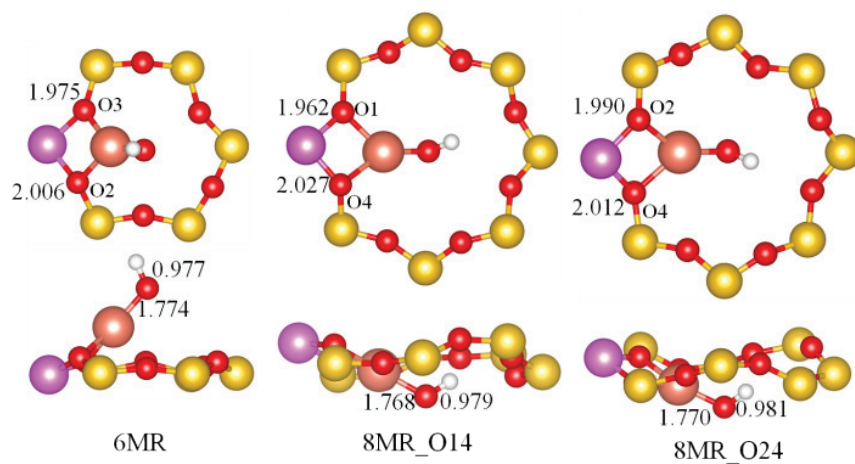
NO<sub>3</sub>\_ZCu



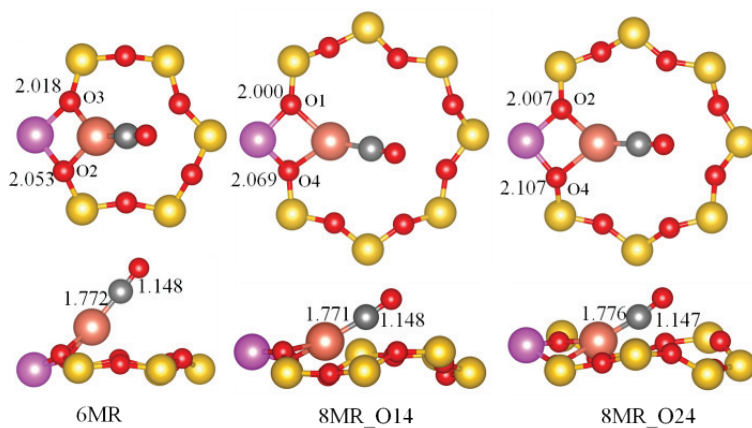
N<sub>2</sub>\_ZCu



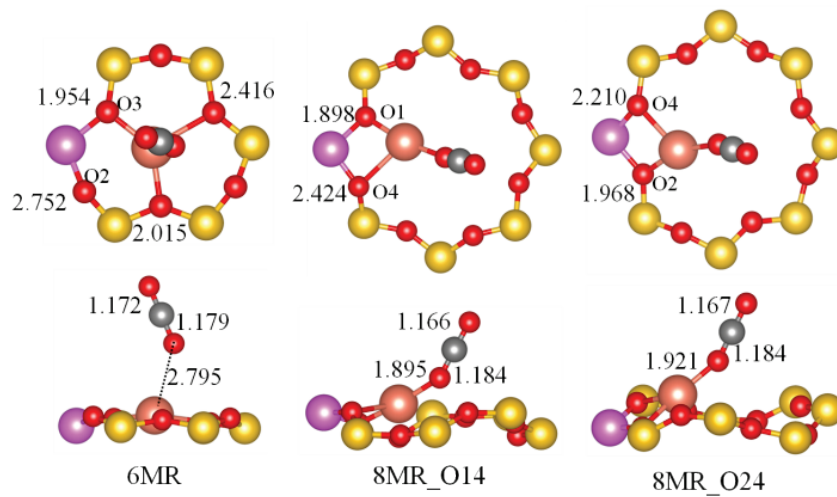
OH\_ZCu



CO\_ZCu



CO<sub>2</sub>\_ZCu



NH<sub>3</sub>\_ZCu

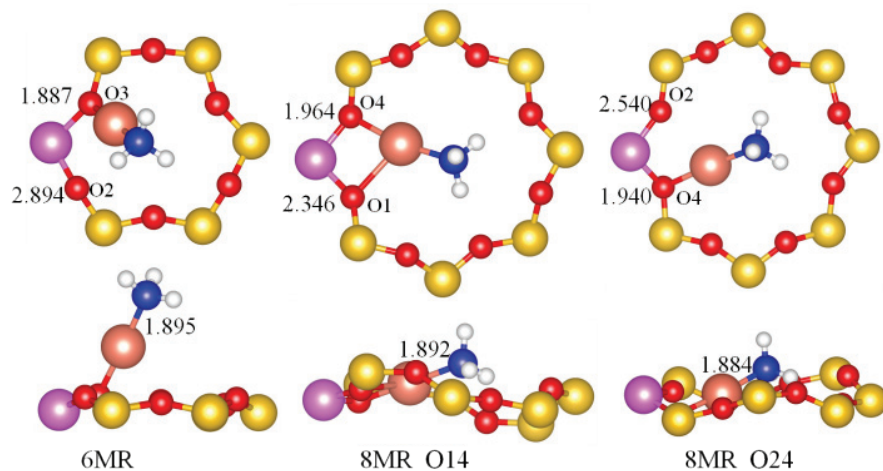


Figure S5. Top and side views of the most favorable local structures of various adsorbates with Cu in different rings (6MR, 8MR\_O14 and 8MR\_O24). The distances between Cu and coordinated atoms are shown. O1, O2, O3 and O4 atoms of the zeolite framework are defined in Figure 1 of main text.

#### 4. Comparison of adsorption energies calculated by using PW91 and HSE06 functionals

Here we compare our PW91 and our HSE06 functional results of the adsorption energies of NO, NO<sub>2</sub> and O<sub>2</sub>. We used the same computational setup to calculate the adsorption energy of NO on a Cu<sup>+</sup> ion and compare our results with the literature in Table S1. All these results are in very good agreement with the results reported by Göttl and Hafner.<sup>2</sup> This demonstrates the reliability of our computational setup.

Table S1. The adsorption energies of NO, NO<sub>2</sub> and O<sub>2</sub> on a Cu<sup>+</sup> site as calculated with the PW91 and the HSE06 functionals. Here the Cu<sup>+</sup> ion is located in different 6MR and 8MR sites. The values in parenthesis are compared to the literature.<sup>2</sup>

E <sub>ads</sub> (eV)	NO		NO <sub>2</sub>		O <sub>2</sub>	
	PW91	HSE06	PW91	HSE06	PW91	HSE06
6MR	-1.27 (-1.30)	-0.87 (-0.89)	-0.97	-0.89	-0.64	-0.43
8MR_O14	-1.78 (-1.71)	-1.28 (-1.16)	-1.44	-1.48	-1.06	-0.53
8MR_O24	-1.70 (-1.88)	-1.19 (-1.20)	-1.56	-1.59	-1.14	-0.59

We note that the total energy differences are independent on the underlying functional while the HSE06 functional decreases the adsorption energies. In our previous work, we also did several comparisons between the PW91 and HSE06 functionals. It is found that the choice of functional doesn't change the total energy difference too much while the HSE06 functional results in a large decrease of adsorption energies as compared to those using the PW91 functional. Details can be found in the section 4 of the Supporting Information of the literature.<sup>3</sup>

## 5. Adsorption of NO<sub>2</sub> on ZCu

As shown in Figure S6, we systematically investigated different configurations of NO<sub>2</sub> adsorbed on ZCu with Cu in 6MR and 8MR sites.

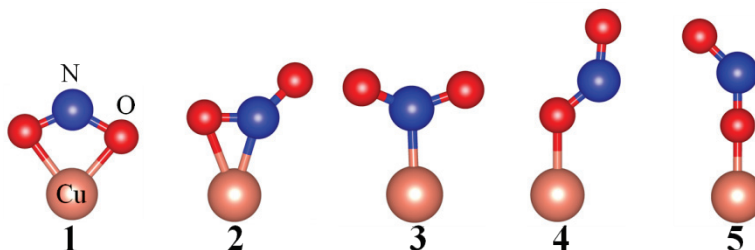


Figure S6. Considered configurations of NO<sub>2</sub> on Cu sites. The atoms of Cu, N and O are labeled.

Table S2. Structure information of NO<sub>2</sub> adsorbed on Cu sites in ZCu, calculated for different Cu locations. Distances are given in Å, angles in degrees and O<sub>N</sub> denotes the O atom in NO<sub>2</sub>.

6MR	Cu-O2	Cu-O3	Cu-N	Cu-O <sub>N</sub>	∠ONO	N-O <sub>N</sub>
config2	1.994	2.004	1.890	2.175	127.1	1.281, 1.210
config4	2.077	2.032, 2.273	-	1.906	123.1	1.284, 1.215
8MR_O14	Cu-O1	Cu-O4	Cu-N	Cu-O <sub>N</sub>	∠ONO	N-O <sub>N</sub>
config1	1.993	1.997	2.440	1.982, 1.992	108.7	1.286, 1.282
config2	1.976	2.025	1.897	2.124	126.9	1.285, 1.208
config4	2.074	1.967	-	1.835	121.7	1.309, 1.201
8MR_O24	Cu-O2	Cu-O4	Cu-N	Cu-O <sub>N</sub>	∠ONO	N-O <sub>N</sub>
config1	2.016	1.981	2.445	1.991, 1.989	108.6	1.286, 1.283
config2	1.967	2.035	1.872	2.312	127.6	1.266, 1.216
config4	2.052	1.976	-	1.825	121.8	1.304, 1.201
NO <sub>2</sub> in gas phase	-	-	-	-	133.7	1.213

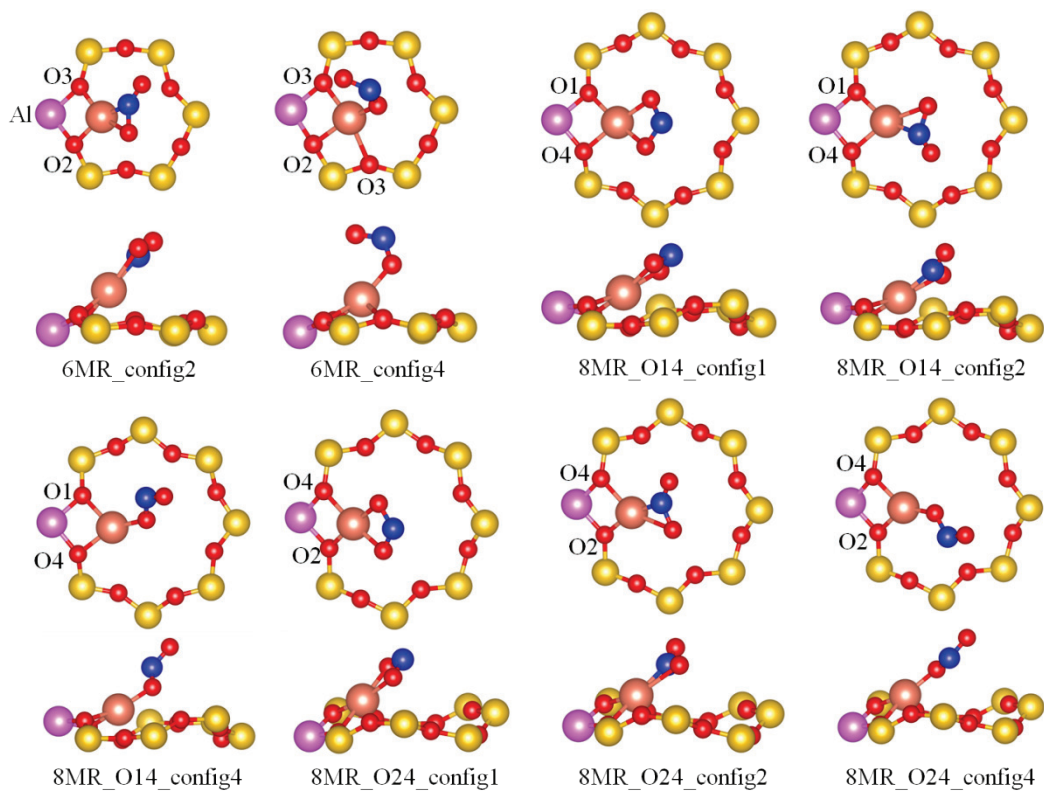


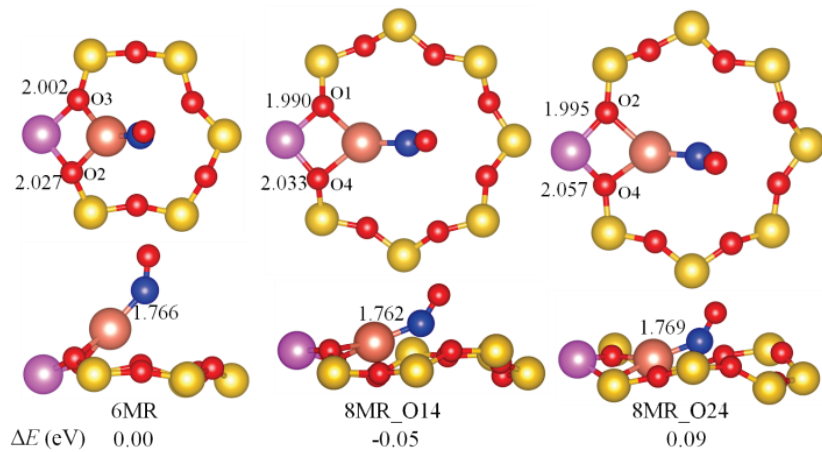
Figure S7. The stable configurations of NO<sub>2</sub> adsorbed on ZCu. Structural information is listed in Table S2.

Table S3. Energies of NO<sub>2</sub> adsorbed on Cu sites in ZCu. Different configurations are shown in Figure S7.  $\Delta E$  is the total energy variation with respect to the total energy of configuration 6MR\_config2.

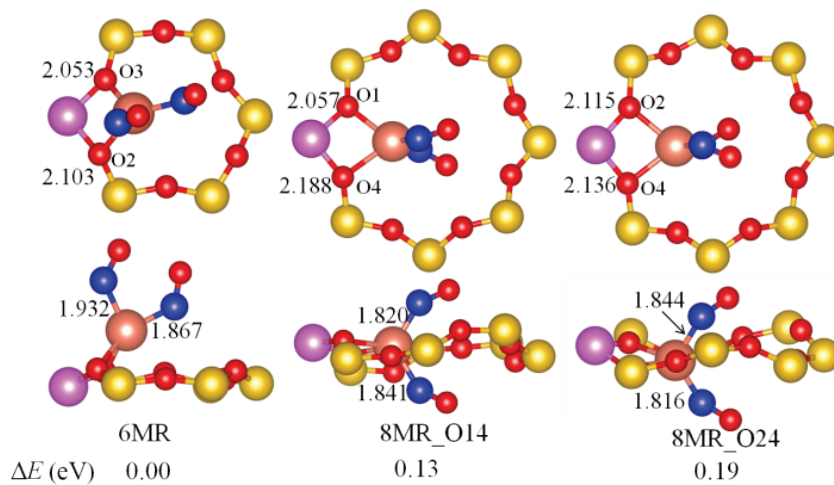
Configurations	$\Delta E$ (eV)	$E_{\text{ads}}$ (eV)
6MR_config2	0.00	-0.97
6MR_config4	0.21	-0.76
8MR_O14_config1	-0.01	-1.44
8MR_O14_config2	0.04	-1.39
8MR_O14_config4	0.23	-1.20
8MR_O24_config1	-0.08	-1.56
8MR_O24_config2	-0.04	-1.52
8MR_O24_config4	0.19	-1.29

6. Structures of ZCu with co-adsorption of NO (or CO) with OH and H<sub>2</sub>O

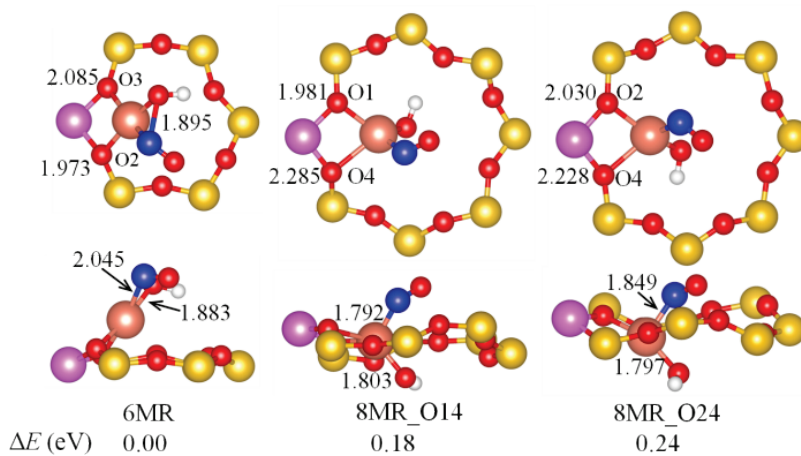
NO\_ZCu



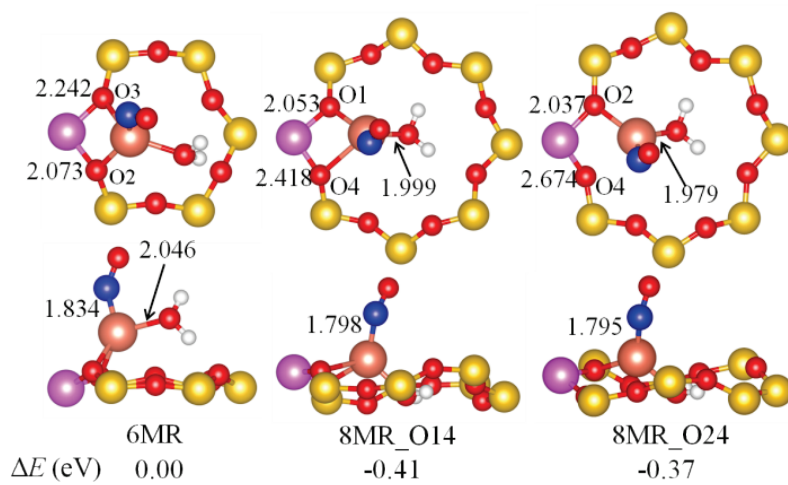
2NO\_ZCu



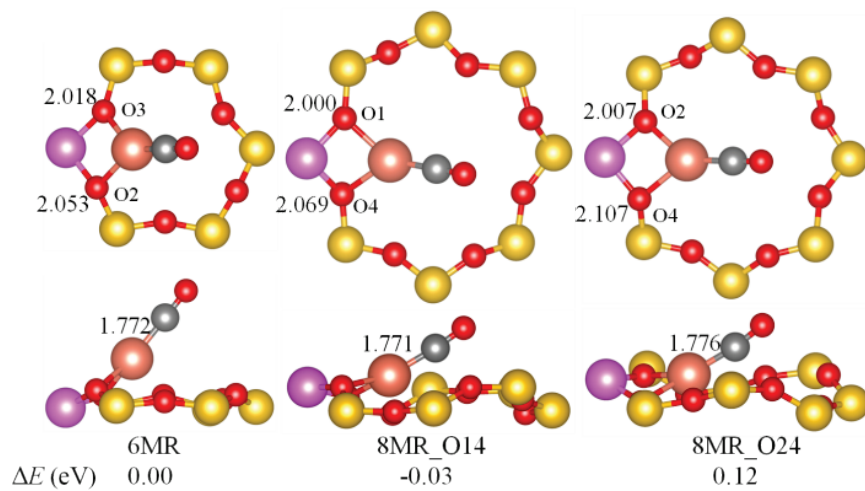
NO+OH\_ZCu



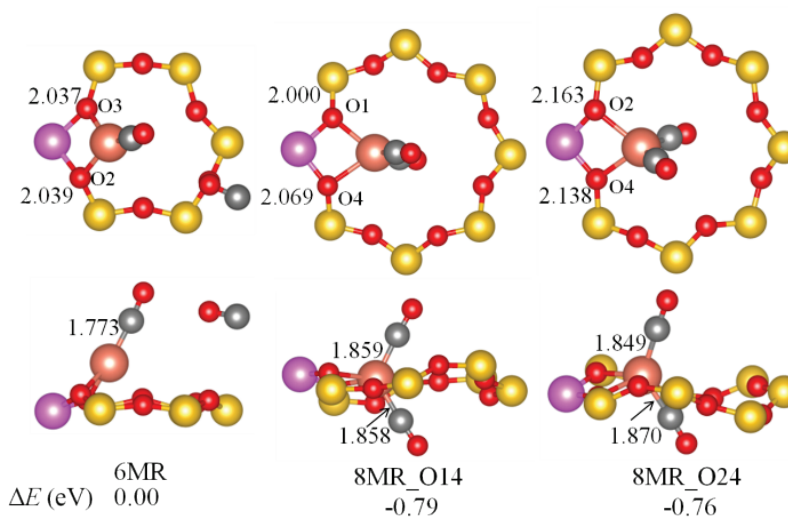
NO+H<sub>2</sub>O\_ZCu



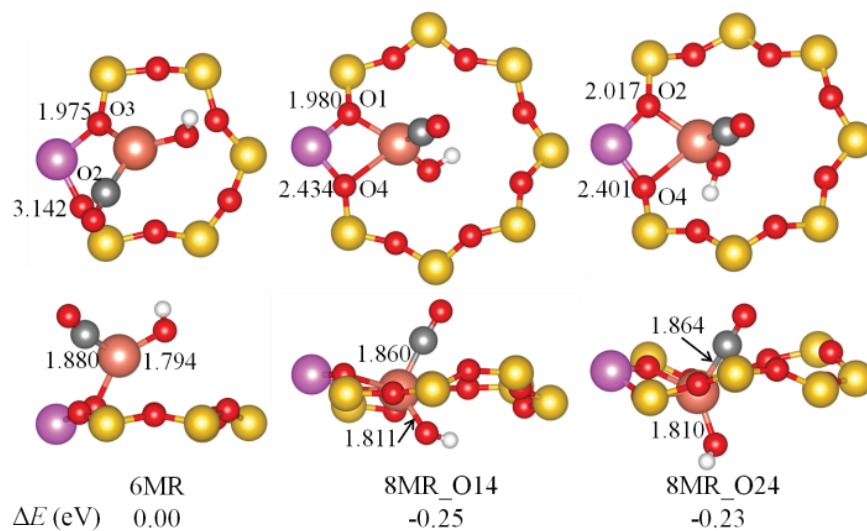
CO\_ZCu



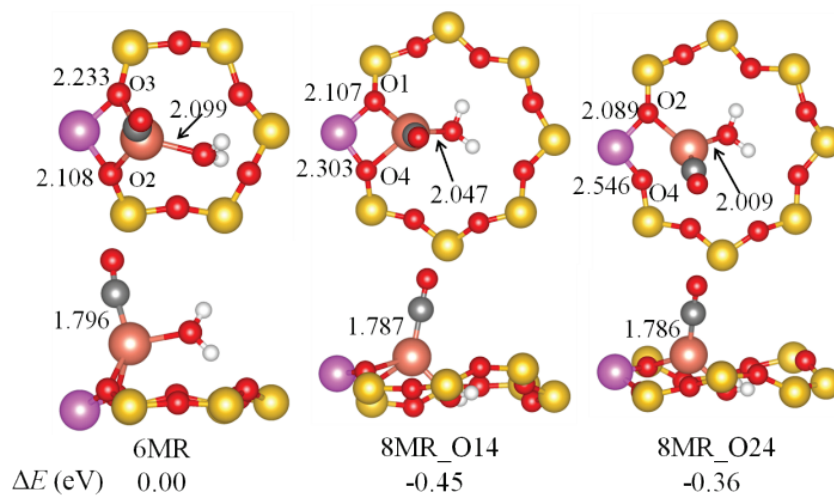
2CO\_ZCu



CO+OH\_ZCu



CO+H<sub>2</sub>O\_ZCu



2OH\_ZCu

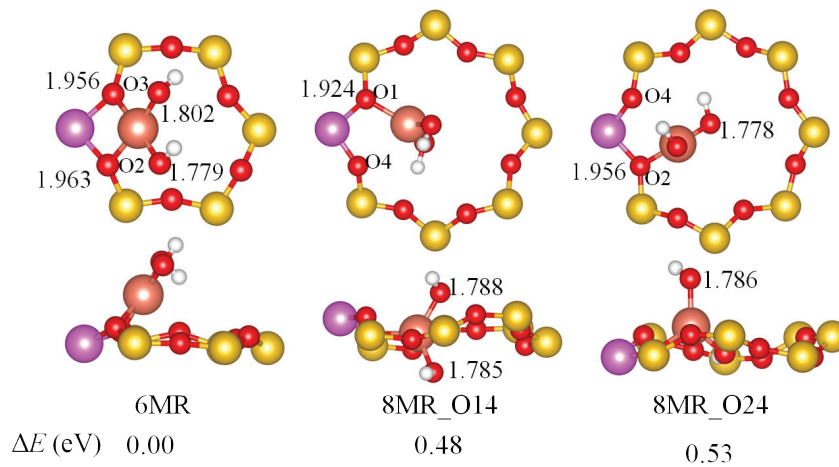
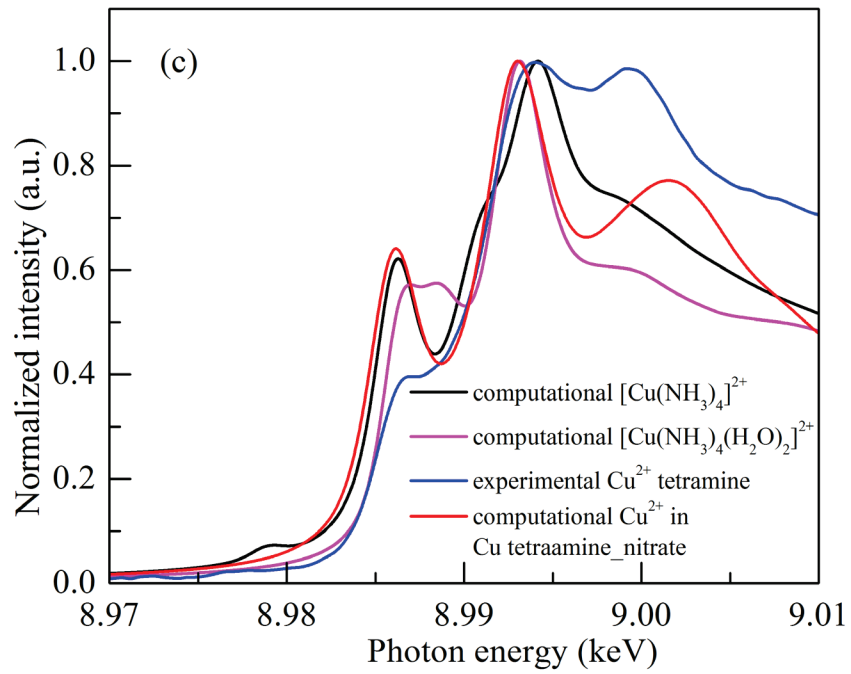
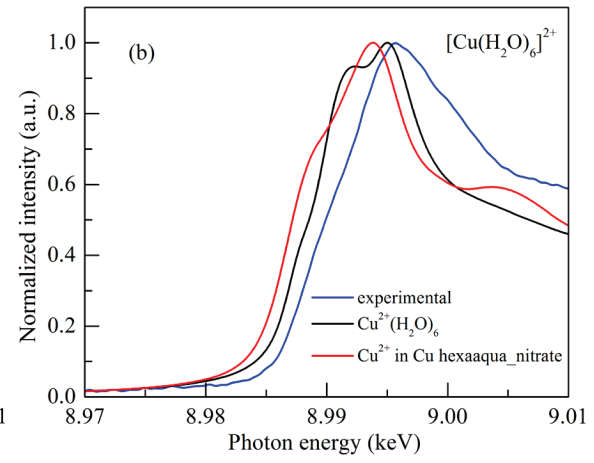
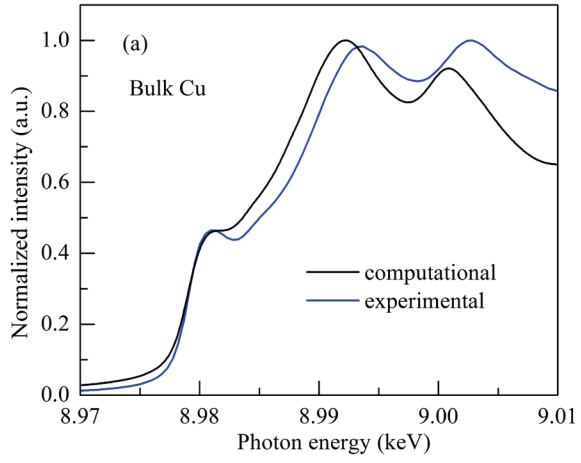


Figure S8. Top and side views of the local structure for Cu in a 6MR, a 8MR\_O14, and a 8MR\_O24 site in the presence of NO (or CO) and other adsorbates. The adsorption of a single NO (or CO) molecule is also shown for comparison. The distances between Cu and the coordinated atoms are shown. O1, O2, O3 and O4 atoms of the oxygen atoms in the zeolite framework are defined in Figure 1 of the main text.  $\Delta E$  is the total energy difference of the adsorbed ZCu conformation with Cu in different sites with respect to Cu in the 6MR site. Positive and negative values of  $\Delta E$  mean that the most favorable site of Cu is in the 6MR and 8MR, respectively.

## 7. Theoretical Cu K-edge XANES calculations

The theoretical K-edge XANES of Cu in bulk Cu, Cu<sub>2</sub>O, CuO, [Cu(NH<sub>3</sub>)<sub>4</sub>]<sup>2+</sup> and [Cu(H<sub>2</sub>O)<sub>6</sub>]<sup>2+</sup> were calculated and the structures we used are shown in Figure 6a. All structures were optimized using the GGA-PBE functional and ultrasoft pseudopotentials. In order to eliminate interactions between periodic images of the core-hole, Cu (3×3×3), Cu<sub>2</sub>O (2×2×2) and CuO (3×3×2) unit cells were used and [Cu(H<sub>2</sub>O)<sub>6</sub>]<sup>2+</sup>, [Cu(NH<sub>3</sub>)<sub>4</sub>]<sup>2+</sup> and [Cu(NH<sub>3</sub>)<sub>4</sub>(H<sub>2</sub>O)<sub>2</sub>]<sup>2+</sup> were placed in a box with a lattice constant of 10 Å, to calculate K-edge XANES of Cu. Instrumental smearing with a Gaussian broadening of 0.6 eV was used in these calculations. As shown in Figure S9a, the computational XANES of bulk Cu has agrees well with the experimental XANES of the Cu foil. As for the experimental XANES of [Cu(H<sub>2</sub>O)<sub>6</sub>]<sup>2+</sup>, the experimental reference XANES is compared to two possible structures. On the one hand, we examined a [Cu(H<sub>2</sub>O)<sub>6</sub>]<sup>2+</sup> complex in a box of 10 Å. We also compared the experimental XANES spectrum to the crystal structure of a Cu<sup>2+</sup> hexaaqua nitrate (as shown in Figure S9d).<sup>4</sup> The experimental and computational XANES spectra are compared in Figure S9b. As for the [Cu(NH<sub>3</sub>)<sub>4</sub>]<sup>2+</sup> reference, three structures are used in our calculations. The first two structures used were [Cu(NH<sub>3</sub>)<sub>4</sub>]<sup>2+</sup> and [Cu(NH<sub>3</sub>)<sub>4</sub>(H<sub>2</sub>O)<sub>2</sub>]<sup>2+</sup>, which were placed in a box of 10 Å. We also compared the XANES spectrum of the experimental reference to the one obtained for the Cu<sup>2+</sup> tetraamine nitrate crystal structure (as shown in Figure S9d).<sup>5</sup> In the work of McEwen *et al.*<sup>6</sup>, the experimental results labeled the Cu<sup>2+</sup> tetraamine reference as [Cu(NH<sub>3</sub>)<sub>4</sub>]<sup>2+</sup>. However, from our computational results shown in Figure S9c, the edge position of Cu K-edge XANES for Cu<sup>2+</sup> tetraamine correlates well with that of Cu in a [Cu(NH<sub>3</sub>)<sub>4</sub>(H<sub>2</sub>O)<sub>2</sub>]<sup>2+</sup> reference. This makes more sense with regard to experiment, since the XANES results for Cu<sup>2+</sup> tetraamine were measured in water solution, where the Cu<sup>2+</sup> tetraamine prefers a [Cu(NH<sub>3</sub>)<sub>4</sub>(H<sub>2</sub>O)<sub>2</sub>]<sup>2+</sup> structure. On the other hand, the computational XANES spectrum of the Cu<sup>2+</sup> tetraamine nitrate structure gives three peaks in its XANES spectrum, in good agreement with the experimental reference.



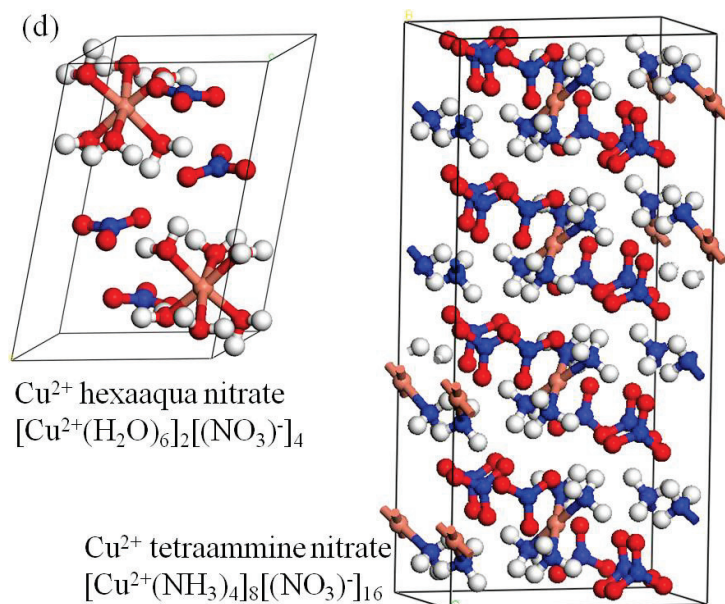


Figure S9. (a) Comparison of the computational and available experimental Cu K-edge XANES for bulk Cu and a Cu foil, respectively. Also shown is a comparison between experimental and computational Cu K-edge XANES for (b)  $[\text{Cu}(\text{H}_2\text{O})_6]^{2+}$  and (c)  $[\text{Cu}(\text{NH}_3)_4]^{2+}$ . (d) Structures of  $\text{Cu}^{2+}$  hexaaqua nitrate<sup>4</sup> and  $\text{Cu}^{2+}$  tetraammine nitrate.<sup>5</sup>

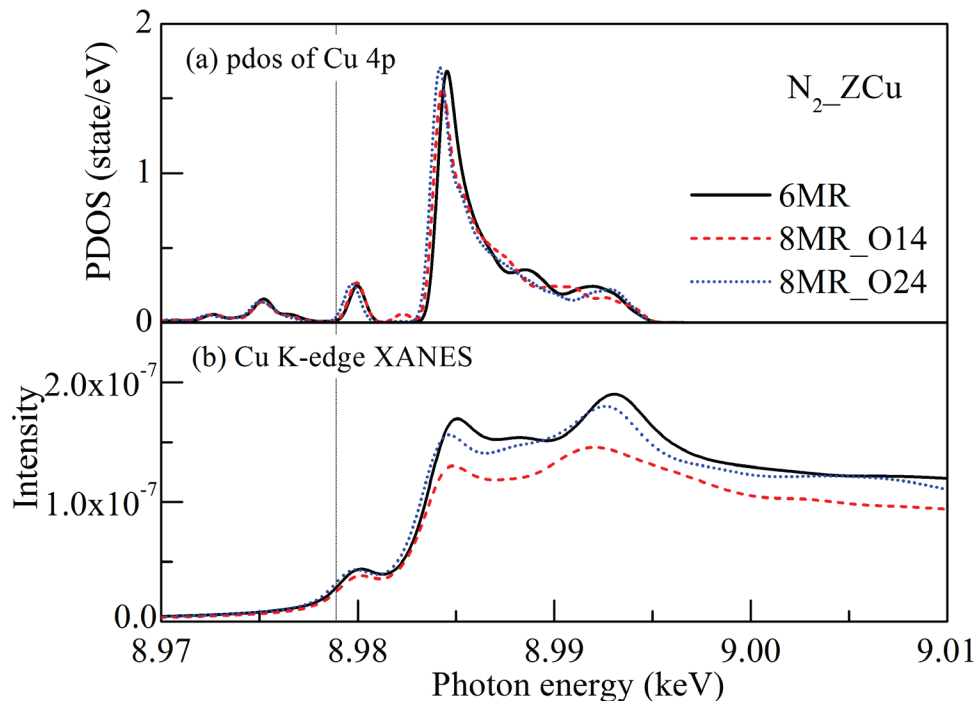
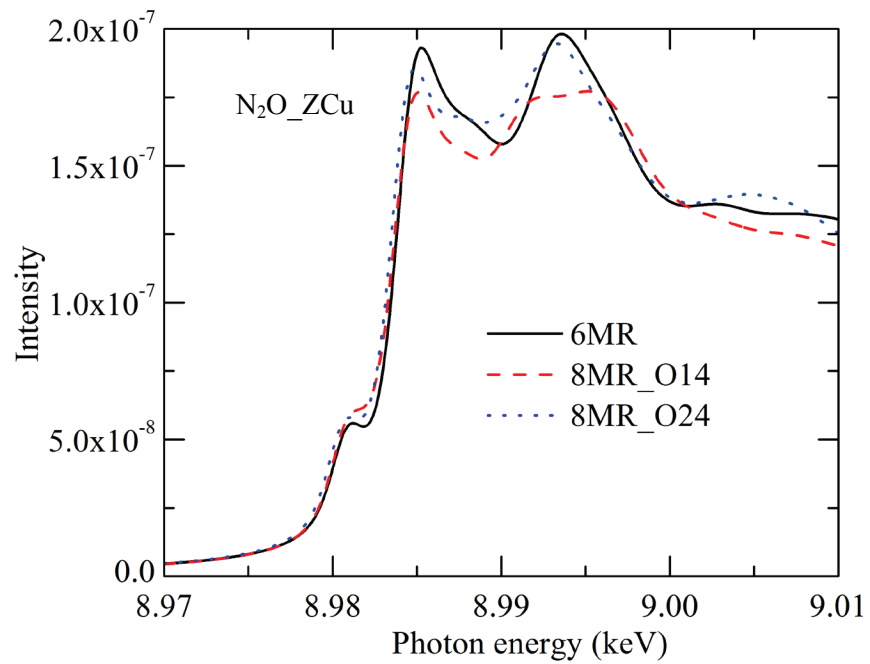
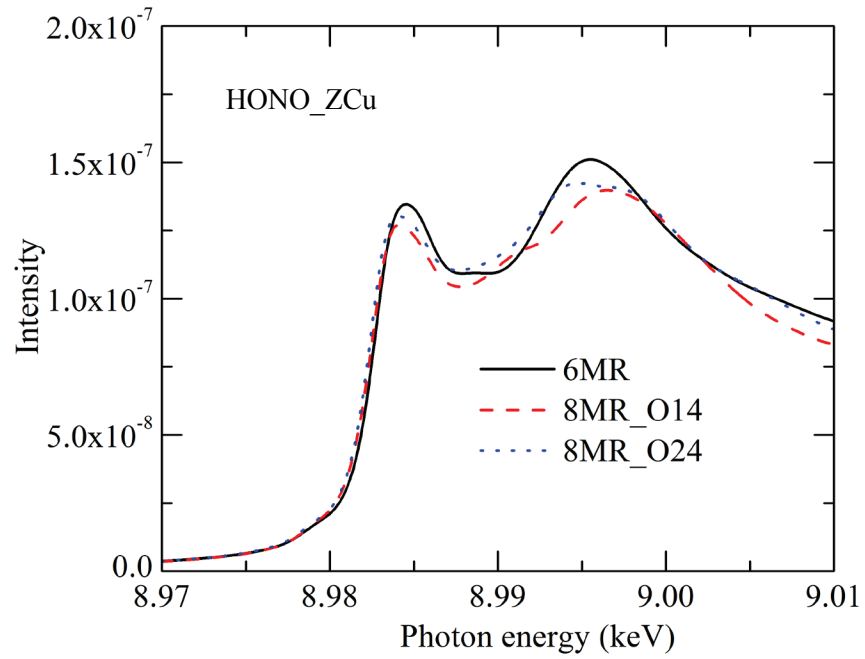
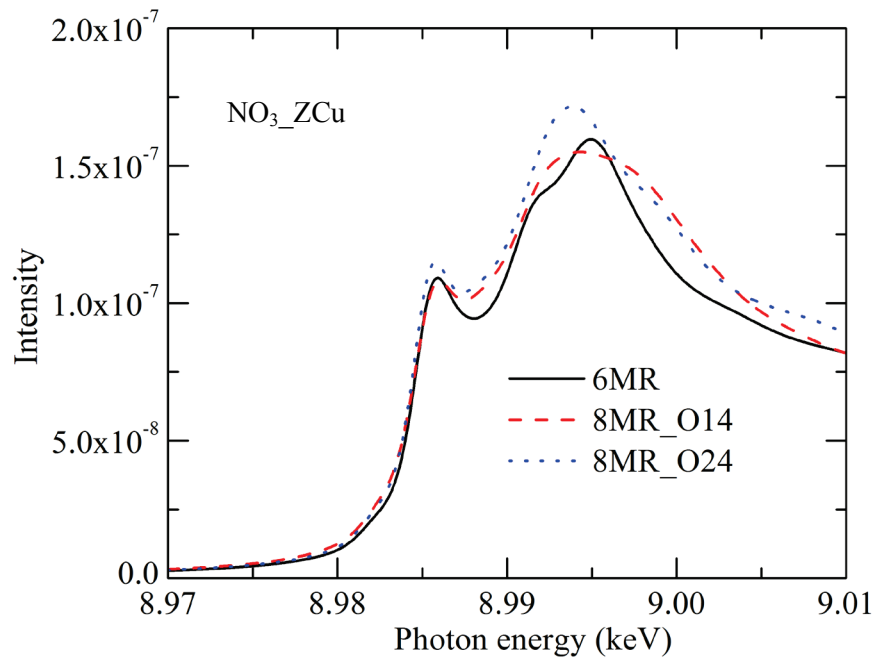
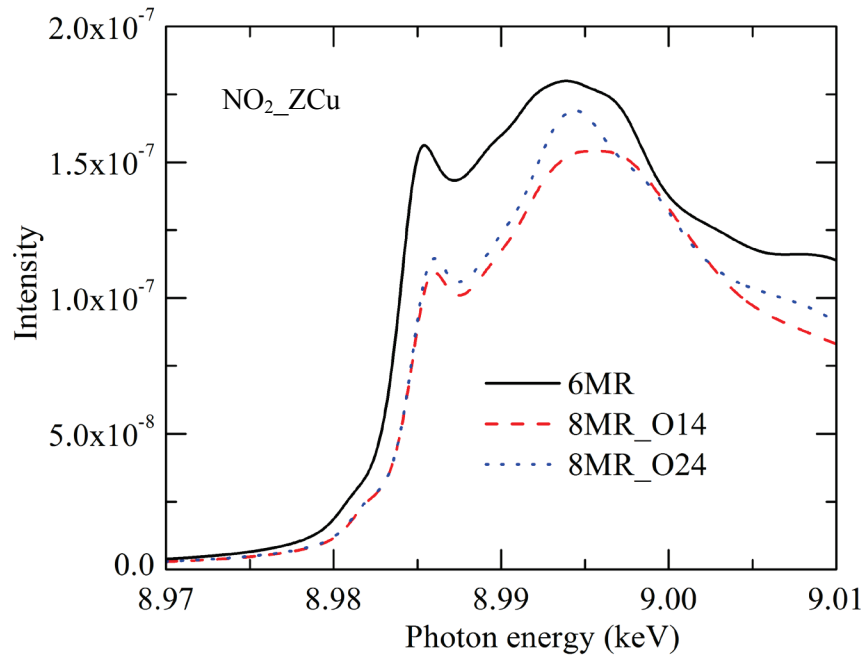


Figure S10. (a) The calculated excited Cu 4p PDOS (b) and computational K-edge XANES of Cu in a 6MR (solid line), a 8MR\_O14 (dashed line) and a 8MR\_O24 (dotted line) location in the presence of  $\text{N}_2$  adsorbed in a ZCu conformation. The vertical dotted line at 8978.9 eV shows the Fermi level.







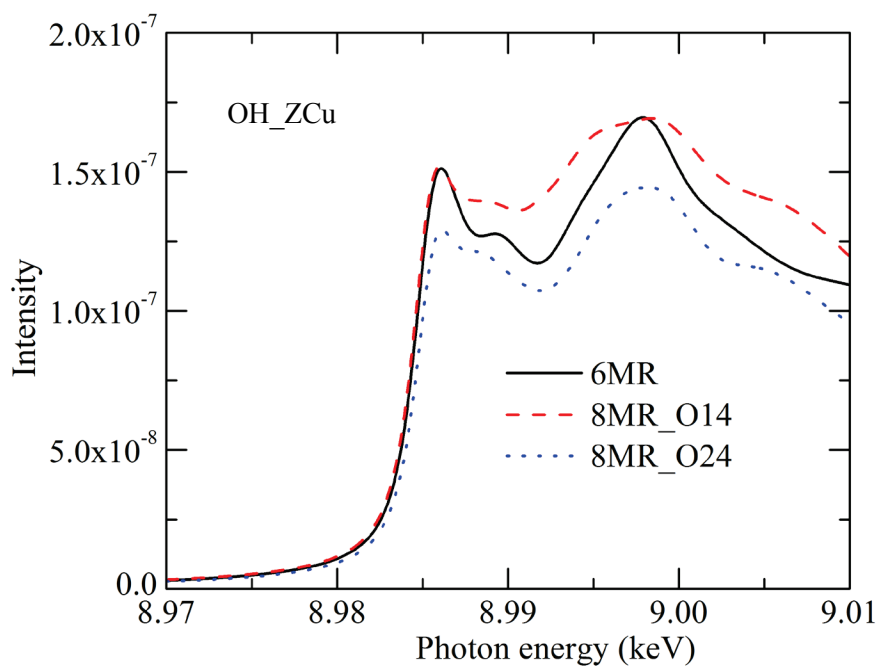
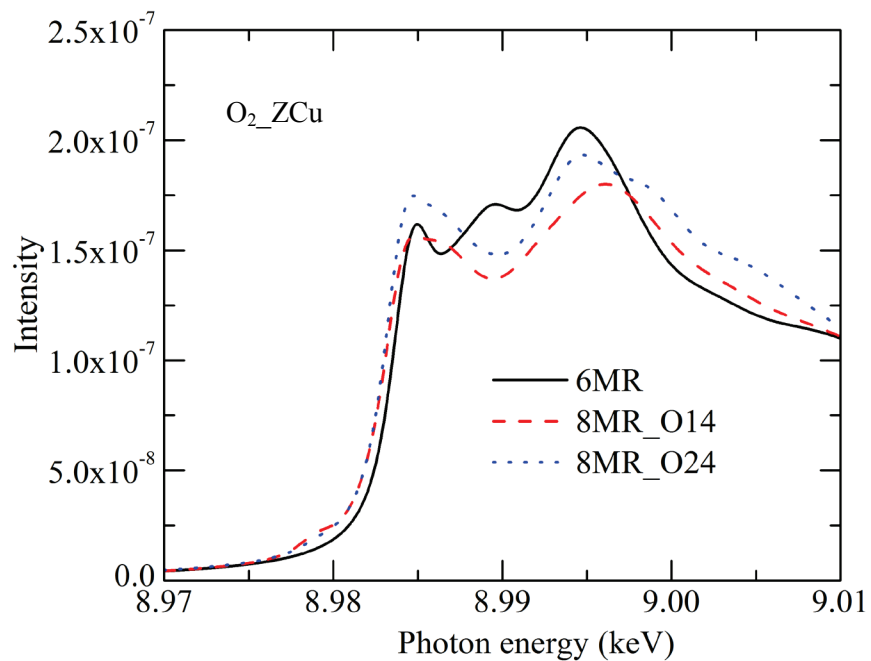


Figure S11. The Cu K-edge XANES for the most stable configurations of HONO\_ZCu, N<sub>2</sub>O\_ZCu, NO<sub>2</sub>\_ZCu, NO<sub>3</sub>\_ZCu, O<sub>2</sub>\_ZCu and OH\_ZCu with Cu in a 6MR (solid line), a 8MR\_O14 (dash line) and a 8MR\_O24 (dotted line) site.

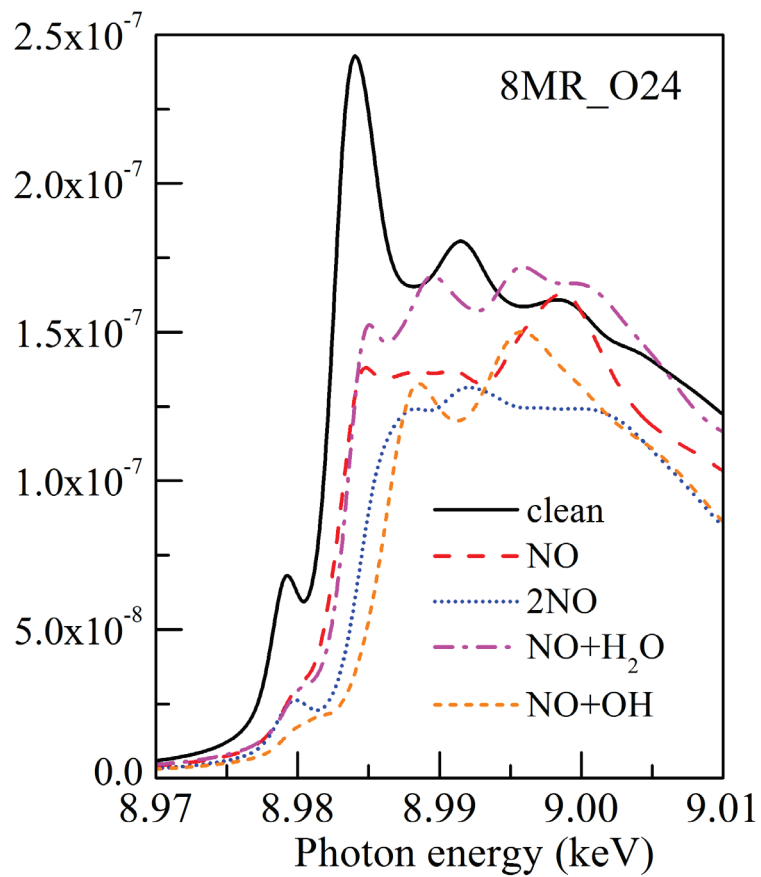


Figure S12. The K-edge XANES of Cu in 8MR\_O24 under different situations, namely, clean, NO adsorption, 2NO adsorption, co-adsorption of NO with water and co-adsorption of NO with OH.

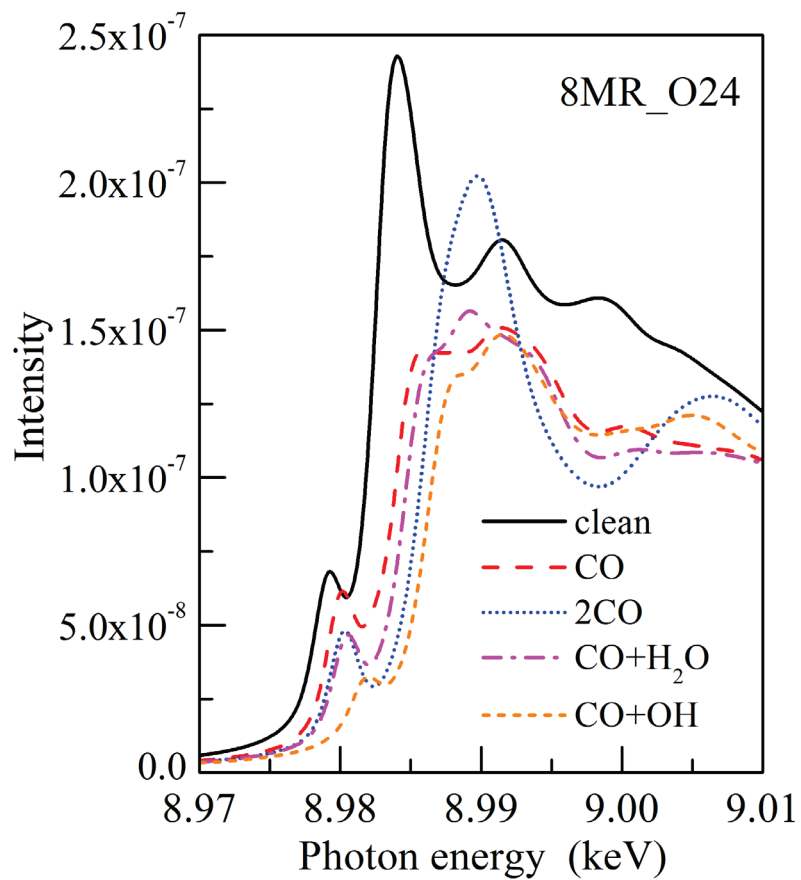


Figure S13. The K-edge XANES of Cu in 8MR\_O24 under different situations, namely, clean, CO adsorption, 2CO adsorption, co-adsorption of CO with water and co-adsorption of CO with OH.

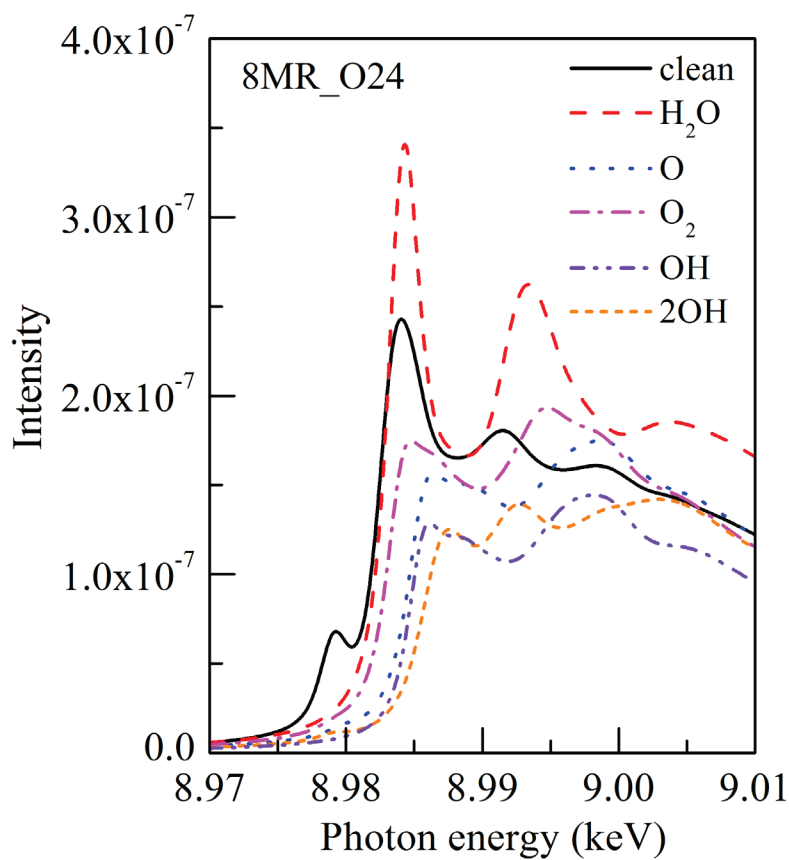


Figure S14. The K-edge XANES of Cu in 8MR\_O24, in the presence of several extra lattice species ( $\text{H}_2\text{O}$ , O atom,  $\text{O}_2$ , OH and 2OH) with different oxidizing power.

Table S4. Edge positions in the computed XANES spectra in the presence of adsorbed molecules in a ZCu conformation (as shown in Figure 18 in the main text) with respect to corresponding clean ZCu conformation with Cu in different locations. Note that the edge position is obtained by differentiating the edge plot and picking the photon energy with highest variation.

Edge position (eV)	clean	$\text{H}_2\text{O}$	$\text{O}_2$	O	OH	2OH
6MR	8983.10	8983.12	8983.72	8984.86	8984.73	8985.00
8MR_O14	8982.60	8983.48	8983.27	8984.71	8984.71	8985.80
8MR_O24	8982.59	8983.29	8983.29	8984.80	8984.81	8985.83

8. Structure of 6  $\text{H}_2\text{O}$  molecules adsorbed in  $\text{Z}_2\text{Cu}$  (hydrated  $\text{Z}_2\text{Cu}$ ) conformation where the  $\text{Cu}^{2+}$  ion is charge compensated by two Al atoms

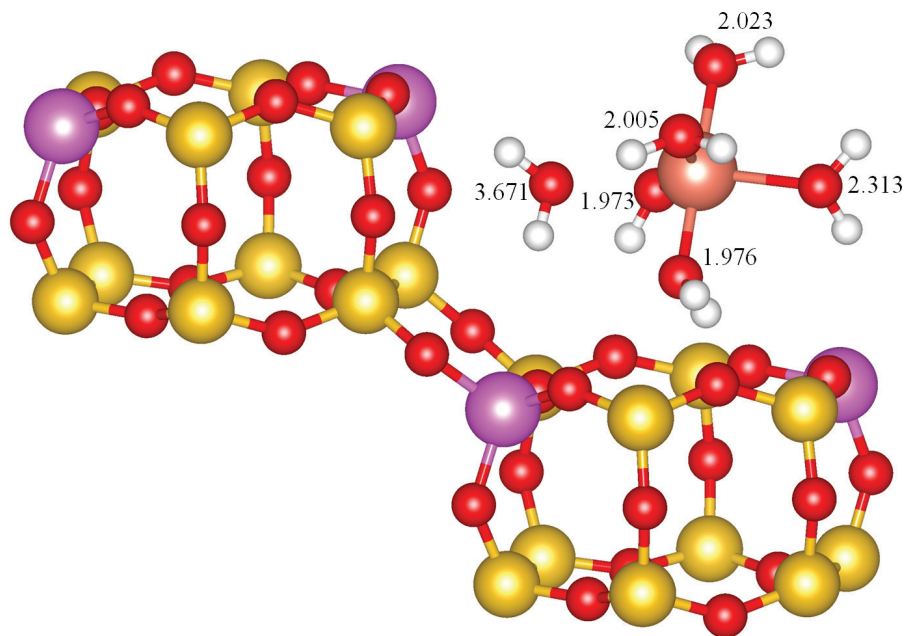


Figure S15. Structure of the  $\text{H}_2\text{O}_6\text{-Z}_2\text{Cu}$  conformation. Five  $\text{H}_2\text{O}$  molecules are coordinated to Cu and another  $\text{H}_2\text{O}$  molecule is close to one of the H atoms of a  $\text{H}_2\text{O}$  molecule that is coordinated with Cu. The distances between the O atom of  $\text{H}_2\text{O}$  and Cu are shown in the figure.

- (1) Prestipino, C.; Bordiga, S.; Lamberti, C.; Vidotto, S.; Garilli, M.; Cremaschi, B.; Marsella, A.; Leofanti, G.; Fisticaro, P.; Spoto, G.; Zecchina, A., *The Journal of Physical Chemistry B* **2003**, *107*, 5022-5030.
- (2) Goltl, F.; Hafner, J., *J. Chem. Phys.* **2012**, *136*, 064503-31.
- (3) Zhang, R.; McEwen, J.-S.; Kollár, M.; Gao, F.; Wang, Y.; Szanyi, J.; Peden, C. H. F., *ACS Catal.* **2014**, *4*, 4093-4105.
- (4) Zibasesht, R.; Hartshorn, R. M., *Acta Cryst.* **2006**, *E62*, i19-i22.
- (5) Morosin, B., *Acta Cryst.* **1976**, *B32*, 1237-1240.
- (6) McEwen, J. S.; Anggara, T.; Schneider, W. F.; Kispersky, V. F.; Miller, J. T.; Delgass, W. N.; Ribeiro, F. H., *Catalysis Today* **2012**, *184*, 129-144.